Whole-exome sequencing of neoplastic cysts of the pancreas reveals recurrent mutations in components of ubiquitin-dependent pathways

Jian Wu[a,1], Yuchen Jiao[a,1], Marco Dal Molin[b,1], Anirban Maitra[b], Roeland F. de Wilde[b], Laura D. Wood[b], James R. Eshleman[b], Michael G. Goggins[b,c], Christopher L. Wolfgang[d], Marcia I. Canto[c], Richard D. Schulick[d], Barish H. Edil[d], Michael A. Choti[d], Volkan Adsay[e], David S. Klimstra[f], G. Johan A. Offerhaus[g], Alison P. Klein[b], Levy Kopelovich[h], Hannah Carter[i], Rachel Karchin[i], Peter J. Allen[j], C. Max Schmidt[k], Yoshiki Naito[l], Luis A. Diaz, Jr.[a], Kenneth W. Kinzler[a], Nickolas Papadopoulos[a], Ralph H. Hruban[b,2], and Bert Vogelstein[a,2]

[a]Ludwig Center for Cancer Genetics and Howard Hughes Medical Institutions, Johns Hopkins Kimmel Cancer Center, Baltimore, MD 21231; Departments of [b]Pathology, [c]Medicine and [d]Surgery, Sol Goldman Pancreatic Cancer Research Center, Johns Hopkins Medical Institutions, Baltimore, MD 21231; [e]Department of Pathology, Emory University, Atlanta, GA 30322; Departments of [f]Pathology and [j]Surgery, Memorial Sloan–Kettering Cancer Center, New York, NY 10065; [g]Department of Pathology, University Medical Center of Utrecht, 3508 GA Utrecht The Netherlands; [h]Division of Cancer Prevention, National Cancer Institute, National Institutes of Health, Bethesda, MD 20892; [i]Department of Biomedical Engineering, Institute for Computational Medicine, The Johns Hopkins University, Baltimore, MD; [k]Departments of Surgery, Biochemistry, and Molecular Biology, Indiana University, Indianapolis, IN 46202; and [l]Department of Pathology, Kurume University School of Medicine, Kurume 830-0011, Japan

Contributed by Bert Vogelstein, November 4, 2011 (sent for review October 12, 2011)

More than 2% of adults harbor a pancreatic cyst, a subset of which progresses to invasive lesions with lethal consequences. To assess the genomic landscapes of neoplastic cysts of the pancreas, we determined the exomic sequences of DNA from the neoplastic epithelium of eight surgically resected cysts of each of the major neoplastic cyst types: serous cystadenomas (SCAs), intraductal papillary mucinous neoplasms (IPMNs), mucinous cystic neoplasms (MCNs), and solid pseudopapillary neoplasms (SPNs). SPNs are low-grade malignancies, and IPMNs and MCNs, but not SCAs, have the capacity to progress to cancer. We found that SCAs, IPMNs, MCNs, and SPNs contained 10 ± 4.6, 27 ± 12, 16 ± 7.6, and 2.9 ± 2.1 somatic mutations per tumor, respectively. Among the mutations identified, E3 ubiquitin ligase components were of particular note. Four of the eight SCAs contained mutations of the von Hippel–Lindau gene (*VHL*), a key component of the *VHL* ubiquitin ligase complex that has previously been associated with renal cell carcinomas, SCAs, and other neoplasms. Six of the eight IPMNs and three of the eight MCNs harbored mutations of *RNF43*, a gene coding for a protein with intrinsic E3 ubiquitin ligase activity that has not previously been found to be genetically altered in any human cancer. The preponderance of inactivating mutations in *RNF43* unequivocally establish it as a suppressor of both IPMNs and MCNs. SPNs contained remarkably few genetic alterations but always contained mutations of *CTNNB1*, previously demonstrated to inhibit degradation of the encoded protein (β-catenin) by E3 ubiquitin ligases. These results highlight the essential role of ubiquitin ligases in these neoplasms and have important implications for the diagnosis and treatment of patients with cystic tumors.

As the result of the increasing use of abdominal imaging in standard medical practice, pancreatic cysts are being identified with increasing frequency. Management of these cysts is concomitantly becoming a major clinical problem (1, 2). Cystic lesions occur in more than 20% of patients examined at autopsy (3), in as many as 19.6% of patients evaluated by MRI (4–6), and in as many as 2.6% of patients evaluated by computed tomography (7, 8). In the vast majority of cases, the cysts are identified as incidental findings in patients undergoing imaging for symptoms unrelated to pancreatic pathology. However, once a cyst is identified, it poses a challenging life-long management problem (1, 2, 9–13). Some cyst types are virtually always benign, some are low-grade malignant, and others are precursors to invasive pancreatic ductal adenocarcinomas (PDAs); PDAs are associated with a dismal prognosis (14–17). The distinction among cyst types is therefore critical for the effective management of patients with pancreatic cysts. Unfortunately, it is often difficult to determine the type of cyst from conventional clinical, radiographic, or cytologic findings (1, 2, 9–17).

Approximately 40% of cysts are nonneoplastic "pseudocysts" that develop as a complication of alcoholic, biliary, or traumatic acute pancreatitis (14–17). They are managed medically or by surgical drainage without resection. The neoplastic cysts (60% of the total cysts) are predominantly of four types: intraductal papillary mucinous neoplasms (IPMNs), mucinous cystic neoplasms (MCNs), serous cystadenomas (SCAs), and solid pseudopapillary neoplasms (SPNs) (18). SCAs, IPMNs, and MCNs are benign (i.e., noninvasive), but IPMNs and MCNs have the potential to progress to PDAs (i.e., become invasive lesions) if not surgically excised (17). Based on the age of patients undergoing surgical resection, some reports have suggested that there is a 5-y lag time from diagnosis of a large noninvasive IPMN (average age of 63.2 y) to diagnosis of an invasive cancer stemming from the IPMN (average age of 68.1 y). This provides a broad time window for curative resection if premalignant cysts are accurately identified (19). SPNs are regarded as low-grade malignant, but they can be cured by surgery if they are detected and removed before their widespread metastasis (20).

IPMNs are the most common type of neoplastic cyst, accounting for ∼25–35% of the total cysts, whereas SCAs, MCNs, and SPNs account for ∼20%, ∼10%, and ∼5% of pancreatic cysts, respectively. SCAs (Fig. 1*A*) are lined by cuboidal glycogen-rich epithelium with centrally placed round nuclei without atypia (17). The epithelium of SCAs is associated with a rich capillary network (21). IPMNs (Fig. 1*B*) arise within the normal ductal system and are lined by columnar mucin-producing cells that often form large papillary projections into ductal lumina (17). MCNs (Fig. 1*C*) are also lined by columnar mucin-producing cells, but in contrast to IPMNs, the neoplastic epithelium is associated with a characteristic ovarian-type stroma and the cysts do not communicate with the ductal system (17). MCNs nearly always occur in the body or tail of the pancreas in women, whereas IPMNs and SCAs can occur in any part of the pancreas and in both sexes. SPNs (Fig. 1 *E* and *F*) are technically solid tumors, but the vast majority of them undergo cystic degeneration that clinically and radiographically

Author contributions: J.W., A.M., L.A.D., K.W.K., N.P., R.H.H., and B.V. designed research; J.W., Y.J., R.F.d.W., N.P., and B.V. performed research; M.D.M., A.M., L.D.W., J.R.E., M.G.G., C.L.W., M.I.C., R.D.S., B.H.E., M.A.C., V.A., D.S.K., G.J.A.O., A.P.K., L.K., P.J.A., C.M.S., Y.N., L.A.D., and R.H.H. contributed new reagents/analytic tools; J.W., Y.J., H.C., R.K., K.W.K., N.P., R.H.H., and B.V. analyzed data; and K.W.K., R.H.H., and B.V. wrote the paper.

The authors declare no conflict of interest.

[1]J.W., Y.J., and M.D.M. contributed equally to this work.

[2]To whom correspondence may be addressed. E-mail: rhruban@jhmi.edu or bertvog@gmail.com.

This article contains supporting information online at www.pnas.org/lookup/suppl/doi:10.1073/pnas.1118046108/-/DCSupplemental.

mimics the other types of pancreatic cystic neoplasms (20). Like MCNs, they generally occur in women and do not communicate with the ductal system. Histologically, SPNs consist of uniform poorly cohesive cells supported by delicate small blood vessels. The neoplastic cells of SPNs do not have a normal counterpart in the normal pancreas.

To date, a definitive diagnosis of neoplastic cyst type can usually only be obtained following histopathological examination of surgically obtained specimens. The decision to resect pancreatic cysts surgically is based on the presumed type of cyst along with clinical parameters. Resection is performed on all cysts that are presumed to be SPNs. In contrast, cysts diagnosed as SCAs only require resection if they cause symptoms. Finally, patients with presumptive MCNs or IPMNs undergo surgery if they meet certain criteria, such as rapid growth or the presence of a mural nodule (1, 2, 9–13). The preoperative diagnosis of surgically excised cysts has been shown to be erroneous in one-third of cases and errors can lead to unnecessary surgical procedures (22). For example, there is no need to excise small asymptomatic SCAs, because they have essentially no malignant potential (17). However, SCAs are sometimes suspected to be IPMNs and therefore surgically excised (1, 2, 22). Major surgical procedures are often required for removal of these cystic lesions; thus, more accurate presurgical diagnosis has the potential to reduce the cost, morbidity, and occasional mortality associated with unnecessary surgery.

Cyst fluids can easily and safely be obtained from patients with pancreatic cysts by endoscopic aspiration (23–28). These fluids are often acellular, and therefore not typically useful for cytological diagnosis. However, such fluids can be analyzed for the presence of biochemical abnormalities, including those of DNA, and have the potential to inform diagnosis and improve the management of patients with these lesions (23–28). To set the stage for future molecular genetics-based diagnostic assays, we have here determined the sequences of the exomes, including all annotated coding genes, of representative cases of all four types of neoplastic cysts.

Results

Experimental Design. Neoplastic cysts are composed of a mixture of neoplastic epithelial cells and nonneoplastic cells [stromal, vascular, and inflammatory (17)] (Fig. 1). To maximize our ability to detect mutations, we carefully microdissected the neoplastic epithelial cells from the nonneoplastic cells. This was most difficult in the MCNs because of the cellular ovarian-type stroma present in these lesions (Fig. 1 *C* and *D*). Following microdissection, the neoplastic cell content of each of the cyst samples analyzed in this study was at least 33%.

DNA from 32 microdissected cysts, 8 of each of the four types, as well as matched DNA from normal tissues of the same patients was used in this study. The clinical and histopathological characteristics of the patients and their cystic lesions are detailed in Dataset S1. The DNA was ligated to adapters and amplified using standard Illumina protocols. The amplified DNA was then captured with a 50-Mb SureSelect Paired-End Target Enrichment System (Agilent). The captured DNA includes more than 20,000 coding genes (http://www.sanger.ac.uk/gencode/) plus all miRNAs in miRBase, v. 13 (http://www.mirbase.org). Sequencing was performed to relatively high depth on an Illumina GAII or HiSeq instrument [average unique coverage of 120-fold ± 40 per base pair in the 64 libraries (32 from cyst DNA and 32 from matched normal DNA), Dataset S2]. This level of sequence coverage confers a >99% probability of detecting clonal heterozygous mutations present in DNA from cyst samples containing >33% neoplastic cells.

Analysis of SCAs. Using SNPs in the sequences captured by the SureSelect Paired-End Target Enrichment System, we were able to identify 15,190 ± 428 heterozygous variants in the matched normal DNA samples of the eight patients with SCAs. Loss of heterozygosity (LOH) of at least one chromosomal region was identified in each of the eight SCAs studied (Fig. 2 and Dataset S3). The maximum degree of LOH (70% ± 13%) confirmed the high fraction of neoplastic cell content achieved on microdissection. The only region that was lost in the majority of SCAs was on chromosome 3p (Fig. 2 and example in Fig. 3*A*). Seven of the eight SCAs lost chromosome 3p alleles, with the losses demarcated by bases 9,934,713–12,850,443. To determine whether this LOH was associated with reduplication of the remaining allele, we compared the copy number of all sequences lying within the regions of LOH with those of all other chromosomal regions in the same cysts. This was accomplished by comparing normalized tag counts through digital karyotyping (29), as explained in *Materials and Methods*. This analysis showed that in all seven SCAs exhibiting LOH of chromosome 3p, only one copy of chromosome 3p sequences remained in the tumor (assuming that the rest of the genome was, on average, diploid rather than polyploid).

We have previously described methods for the reliable identification of somatic mutations in next-generation sequencing data obtained from Illumina instruments (30, 31). Using stringent cri-

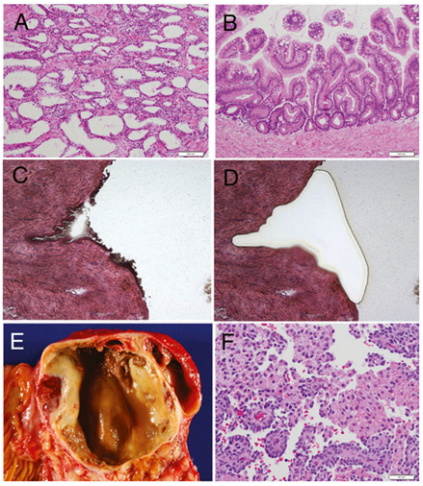

Fig. 1. Neoplastic cyst histopathology. (*A*) Typical SCA (SCA 38) shows centrally placed round nuclei without atypia. (Scale bar: 100 μ.) (*B*) Typical IPMN (IPMN 4) is lined by columnar mucin-producing cells that form large papillary projections into the ductal lumen. (Scale bar: 100 μ.) (*C*) Typical MCN is also lined by columnar mucin-producing cells, but the neoplastic epithelium is associated with a characteristic ovarian-type stroma. (Scale bar: 100 μ.) (*D*) Same MCN after laser capture microdissection of the columnar mucin-producing cells. (Scale bar: 100 μ.) (*E*) Gross appearance of a typical cyst-forming SPN (SPN 2). (Scale bar: 10 mm.) (*F*) Under the microscope, SPN 17 shows poorly cohesive cells supported by a delicate stroma. (Scale bar: 50 μ.)

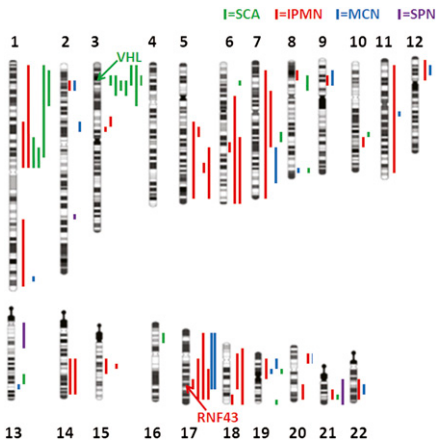

Fig. 2. LOH observed in neoplastic cysts of the pancreas. The lines indicate the observed regions of loss, with the different cyst types denoted by the indicated colors.

teria to avoid false-positive calls, we identified a total of 79 nonsynonymous somatic mutations distributed within 71 genes among the eight SCA tumors (Dataset S4). There was an average of only 10 ± 4.6 nonsynonymous somatic mutations per tumor, far less than observed in PDAs [48 ± 23 per tumor (32); $P < 0.001$].

There were only two genes mutated in more than one SCA (Dataset S4). One of these was TBC1 domain family member 3F (*TBC1D3*), in which two missense mutations were observed (Dataset S4). This gene encodes a protein that stimulates the GTPase activity of RAB5A, which is important for early endosome trafficking (33, 34). Oncogenic properties of TBC1D3 have been demonstrated previously in vitro and in mouse models, and the *TBC1D3* locus is amplified in 15% of primary prostate tumors (35) (36). However, whether the two *TBC1D3* mutations we identified are drivers or passengers (defined as mutations that did or did not directly contribute to oncogenesis, respectively) is not known. In contrast, the von Hippel–Lindau gene (*VHL*) located on chromosome 3p at position 10,158,319–10,168,746, is a bona fide tumor suppressor gene (37), and four of the SCAs contained mutations in this gene [N78S in SCA 23, W117L in SCA 35, C162W in SCA 38, and S80R in SCA 40 (Dataset S4)]. Three of these four (SCA 23, SCA 38, and SCA 40) showed evidence of LOH of the *VHL* chromosomal region (Dataset S3). Interestingly, the four tumors without detectable mutations of *VHL* (SCA 14, SCA 27, SCA 29, and SCA 37) had lost one allele of chromosome 3p within or adjacent to *VHL* (Fig. 2 and Dataset S3). We speculate that in these four cases, the *VHL* gene was inactivated by genetic alterations, such as deletions or translocations not detectable by sequencing, or by epigenetic mechanisms such as those responsible for *VHL* silencing in renal cell carcinomas (RCCs) (38).

SCAs have been identified in more than 15% of patients with *VHL* syndrome, a disease that predisposes to RCCs and other tumor types (39, 40). Of note, SCAs share several histomorphological characteristics with RCCs, including excessive glycogen production and a distinctive recruitment of vasculature (angiogenesis). All four mutations in *VHL* identified in SCAs were identical to ones previously identified in RCCs (http://www.sanger.ac.uk/genetics/CGP/cosmic/); three of the four were identical to ones previously described in the germline of patients with *VHL* syndrome, and the fourth (W117L) was at the same amino acid position found to be mutated in the germline of patients with *VHL* syndrome. This provides conclusive evidence of the inactivating nature of these mutations in human cells. In each of these four cases, we additionally confirmed that the *VHL* mutations in the cysts were somatic using independent ligation-based assays (Fig. 4 *A* and *B*).

To our knowledge, no mutations of *VHL*, or any other gene, have been identified in the fluids obtained from SCA cysts. Demonstration of such mutations in samples obtained by fine needle aspiration could be useful from a diagnostic standpoint, as discussed above. To determine whether *VHL* mutations could be identified in the fluids from SCAs, we designed a customized chip containing *VHL* gene sequences and used it to capture libraries from the DNA of 18 SCA cyst fluids. In nine (50%) of these cases, we identified point mutations in *VHL* (Dataset S5). Four of the mutations were predicted to inactivate the encoded protein's function, because two produced nonsense codons, one was a 1-bp deletion producing a frameshift, and one altered the splice donor site. Of the five missense mutations, four were identical to those observed in the germline of patients with *VHL* syndrome. Similar capture of *VHL* genes from 28 IPMNs and three MCNs revealed no *VHL* mutations.

Analysis of IPMNs. In a previous study, in which we analyzed 169 well-annotated cancer genes, we identified recurrent mutations of Guanine nucleotide binding protein (G protein), alpha stimulating activity polypeptide 1 (*GNAS*) and v-Ki-ras2 Kirsten rat sarcoma viral oncogene homolog (*KRAS*) in IPMN samples and showed that these mutations were present in 66% and 81% of IPMNs, respectively (41). *KRAS* mutations had previously been identified in IPMNs as well as in PDAs (42, 43) To extend these analyses, we performed whole-exome sequencing on DNA from eight microdissected high-grade IPMNs and matched normal tissues.

LOH of at least one chromosomal region was identified in seven of the eight IPMNs (Fig. 2 and Dataset S3). No losses of the region

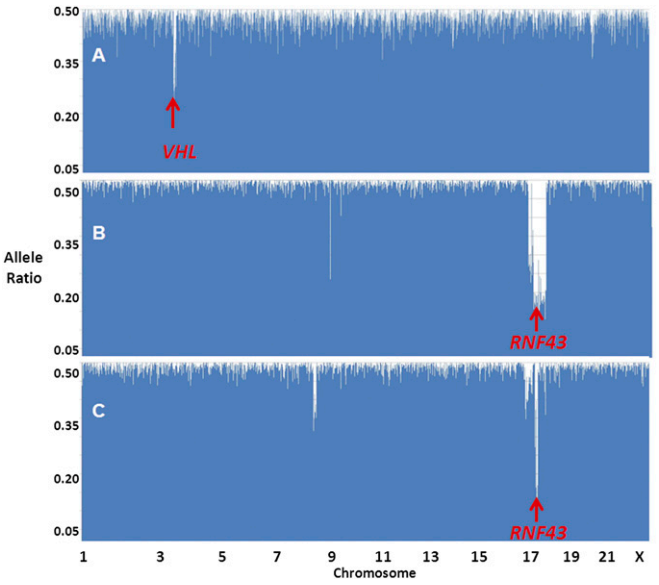

Fig. 3. Representative LOH data based on the sequence evaluation of genome-wide SNPs. The positions of each chromosome are indicated on the *x* axis. The *y* axis indicates the ratio of the two alleles of each SNP. In normal cells, this fraction is 0.5; in a pure neoplastic cell population in which every cell loses one allele of a locus, the allele ratio is 0.0. At a locus at which at least some neoplastic cells had undergone LOH, allele ratios greater than 0.0 reflect nonneoplastic cells that "contaminated" the microdissected cell population plus the fraction of neoplastic cells that had not undergone LOH at that locus. (*A*) SCA 40, exhibiting LOH of the region on chromosome 3p containing the *VHL* gene. (*B*) IPMN 12, exhibiting LOH of the region on chromosome 17q containing the *RNF43* gene. (*C*) MCN 169, exhibiting LOH of the region on chromosome 17q containing the *RNF43* gene.

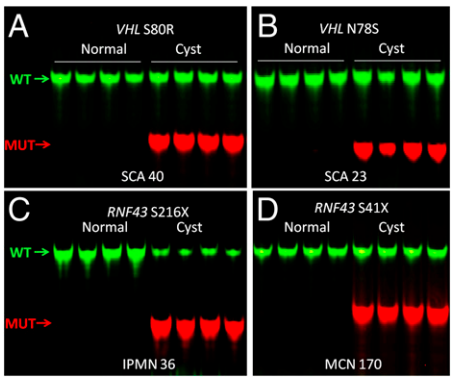

Fig. 4. Ligation assays used to confirm mutations in *VHL* and *RNF43*. Each lane represents the results of ligation of one of four independent PCR products, with each containing 100 template molecules. The ligation products were then size-separated on a denaturing acrylamide gel. The green bands are 6-carboxyfluorescein–labeled oligonucleotide probes that ligate to an unlabeled oligonucleotide when WT alleles are present. The red bands are hexachlorofluorescein-labeled oligonucleotide probes that ligate to the same unlabeled oligonucleotide only when mutant (MUT) alleles are present. The WT- and MUT-specific oligonucleotide probes were of different lengths (~32 and ~12 bases, respectively); thus, they migrated at different positions in the acrylamide gel. The cyst samples and mutations assessed are indicated.

Table 1. Recurrent genetic alterations in neoplastic cysts of the pancreas

Cyst type	Sample ID	*VHL*	*RNF43*	*KRAS*	*GNAS*	*CTNNB1*
SCA	SCA 14	LOH	None	None	None	None
SCA	SCA 23	LOH, p.N78S	None	None	None	None
SCA	SCA 27	LOH	None	None	None	None
SCA	SCA 29	LOH	None	None	None	None
SCA	SCA 35	LOH, p.W117L	None	None	None	None
SCA	SCA 37	LOH	None	None	None	None
SCA	SCA 38	p.C162W	None	None	None	None
SCA	SCA 40	LOH, p.S80R	None	None	None	None
IPMN	IPMN 4	None	None	None	p.R201C	None
IPMN	IPMN 11	None	LOH, p.R145X	p.G12D	p.R201C	None
IPMN	IPMN 12	None	LOH, p.Y177X	None	p.R201C	None
IPMN	IPMN 20	None	p.Q152X	p.G12D	p.R201C	None
IPMN	IPMN 21	None	LOH, p.R371X	p.G12D	p.R201H	None
IPMN	IPMN 26	None	None	p.G12R	None	None
IPMN	IPMN 36	None	LOH, p.S216X	p.G12R	None	None
IPMN	IPMN 41	None	p.R113X	None	None	None
MCN	MCN 158	None	None	None	None	None
MCN	MCN 162	None	None	p.G12V	None	None
MCN	MCN 163	None	None	p.G13D	None	None
MCN	MCN 164	None	None	p.G12V	None	None
MCN	MCN 166	None	p.R371X	p.G12D	None	None
MCN	MCN 168	None	LOH, p.R127P	p.G12V	None	None
MCN	MCN 169	None	LOH	None	None	None
MCN	MCN 170	None	p.S41X	p.G12V	None	None
SPN	SPN 2	None	None	None	None	p.G34R
SPN	SPN 4	None	None	None	None	p.S33C
SPN	SPN 5	None	None	None	None	p.D32H
SPN	SPN 6	None	None	None	None	p.D32A
SPN	SPN 8	None	None	None	None	p.S37F
SPN	SPN 12	None	None	None	None	p.G34V
SPN	SPN 17	None	None	None	None	p.G34R
SPN	SPN 19	None	None	None	None	p.D32N

containing the *VHL* gene were identified. The most commonly deleted region was on chromosome 17q, demarcated by nucleotides 53,790,884–53,939,507, which was observed in four of the eight samples (Fig. 2, Dataset S3, and example in Fig. 3*B*). Digital karyotyping showed that in these four cases, the LOH events were not associated with reduplication of the deleted chromosome 17q region.

Using the same criteria described above for SCAs to identify somatic mutations, a total of 211 nonsynonymous mutations within 191 genes were identified among the eight IPMNs (Dataset S4). There were 26 ± 12 nonsynonymous somatic mutations per tumor (Dataset S2), which is more than twice the number found in SCAs ($P < 0.001$) and approximately half as many as found in PDAs ($P < 0.001$).

There were six genes that were mutated in more than one of the eight IPMNs (Dataset S4). As expected, both *KRAS* and *GNAS* mutations were common, each identified in five tumors and always at codons 12 and 201, respectively (Dataset S4). Two mutations in Adenomatous polyposis coli (*APC*) were observed. *APC* is a well-known tumor suppressor gene whose mutations usually initiate colorectal tumorigenesis (44). One of the *APC* mutations was a nonsense base substitution (R450X in IPMN 4), typical of the inactivating mutations that occur in the germline of patients with colorectal cancers. The second was a missense substitution (R99W in cyst 21) whose functional effects, if any, are unknown. Two different IPMNs had mutations in oligonucleotide/oligosaccharide-binding fold containing 1 (*OBFC1*), and two others had mutations in calcium channel, voltage-dependent, T type, α-11 subunit (*CACAN11*). There are no genetic or functional data implicating these two genes in neoplastic processes. Cancer-specific high-throughput annotation of somatic mutations (CHASM) analysis (45), which determines the probability that a given mutation alters the structural or biochemical properties of a protein, showed that the missense mutations in *OBFC1* and *CACAN11*, as well as the one in *APC*, were not very likely to alter the function of the encoded proteins and may have been passengers. The CHASM scores of all missense mutations identified in this study are provided in Dataset S3.

The most commonly mutated gene in IPMNs was *RNF43*, which is located on chromosome 17, nucleotides 53,786,037–53,849,930, within the small region of chromosome 17q experiencing LOH in IPMNs (Dataset S3). The protein encoded by *RNF43* has been shown to have intrinsic E3 ubiquitin ligase activity (46). *RNF43* was mutated in six of the eight tumors, including all four that had undergone chromosome 17q LOH. Five of the six mutations were base pair substitutions resulting in nonsense codons (Dataset S4). Based on the number and type of mutations in this gene, the probability that it functioned as a passenger was extremely low ($<10^{-12}$, binomial test). Each of the six *RNF43* mutations was confirmed by an independent ligation-based assay (example in Fig. 4*C*). Although expression of *RNF43* has been shown to be correlated with increased cell growth (47), the inactivating mutations of this gene in IPMNs leave little doubt that it suppresses neoplasia in pancreatic ductal epithelial cells.

Analysis of MCNs. Relatively few LOH events were identified in the MCNs compared with the IPMNs (Fig. 2 and Dataset S3). Only one region was lost in more than one tumor, and this region was on chromosome 17q and included the *RNF43* gene (Fig. 3*D*).

A total of 128 nonsynonymous somatic mutations distributed within 115 genes were identified among the eight MCNs (Dataset S4). There were 16.0 ± 7.6 nonsynonymous somatic mutations per tumor, more than in SCAs but less than in IPMNs (Dataset S2). Three MCNs harbored intragenic mutations in *RNF43*, including

one of the two tumors with LOH of the *RNF43* locus. Two of the alterations were nonsense mutations (S41X and R371X), and the third was a missense mutation (R127P) (Dataset S4). This type of mutational pattern, with an overrepresentation of inactivating mutations, is characteristic of tumor suppressor genes and is similar to that observed for *RNF43* in IPMNs (Table 1). One of the MCNs with a truncating mutation was a low-grade MCN (MCN 166), whereas the other two tumors with *RNF43* mutations were high-grade MCNs.

In addition to these *RNF43* mutations, *KRAS* mutations were found in six MCNs and *TP53* mutations were found in two. The *KRAS* mutations were all at codon 12, in accord with previous studies of MCNs (41, 48). The *TP53* alterations were identical to those observed previously in other cancer types (http://www.sanger.ac.uk/genetics/CGP/cosmic/). Because *TP53* mutations are often associated with aggressiveness, it is possible that the MCNs with mutations in this gene are the ones most likely to progress to PDAs. Finally, there were two other genes (*MUC4* and *POTEJ*) that were mutated in more than one MCN, but analysis of the mutations by CHASM did not suggest that they would have substantial effects on protein function (Dataset S4).

Analysis of SPNs. The most notable finding about SPNs was the paucity of genetic alterations identified. Only one of the eight tumors studied exhibited any LOH whatsoever (Figs. 2 and 3 and Dataset S3). The absence of LOH was not attributable to contamination of the microdissected samples with nonneoplastic cells; this possibility could be excluded both by histopathological analysis and by the high fraction of *CTNNB1* mutant alleles, as discussed below (39–59%, Dataset S4).

As with LOH, the number of point mutations was also very low (2.9 ± 1.8 mutations per tumor). This number is lower than any of the other cyst types ($P < 0.001$) and, indeed, is less than any tumor type yet evaluated by genome-wide sequencing (49, 50), including pediatric tumors (51). Five of the eight tumors contained only one or two somatic mutations (Dataset S4). Nevertheless, every tumor had a missense mutation of *CTNNB1*, and all these mutations were at codon 32, 33, 34, or 37. This region of the encoded protein (β-catenin) is critical for regulation of the protein (52–54). When phosphorylated at serine or threonine residues lying between codons 32 and 37, β-catenin is degraded by E3 ubiquitin ligases. Mutations within this region inhibit phosphorylation and the consequent degradation of the protein (55, 56). Previous studies have shown that *CTNNB1* is nearly always mutated in SPNs (57, 58). Our study shows that the *CTNNB1* mutations are the only mutations that are evident in these tumors in many cases, even when all coding genes are assessed by sequencing. An evaluation of these tumors for translocations or epigenetic events may lead to the identification of additional alterations. If not, this tumor type would represent an exception to the widely held view that several sequential mutations are required for the formation of solid tumors in adults (59).

Discussion

The results described above have implications for both basic and applied research. It is fascinating that all four types of cysts are associated with defects in genes that are either components of ubiquitin ligase complexes (SCAs, IPMNs, and MCNs) or render them resistant to degradation by such complexes (SPNs). *RNF43*, genetically inactivated in both types of mucinous cysts (IPMNs and MCNs), has intrinsic E3 ubiquitin ligase activity (46). There has been relatively little research on this gene's product, although it has been shown to be present in a complex that regulates p53-mediated apoptosis (60). Based on these past studies, it is likely that the tumor suppressor effects of the WT *RNF43* gene product are a result of its ubiquitin ligase activity. To confirm this hypothesis, it will be important to determine the proteins that RNF43 ubiquinates in vivo as well as to demonstrate that such ubiquitination is essential for its tumor-suppressive role.

In contrast, *VHL* has been the subject of intense research since its identification as the gene responsible for *VHL* syndrome (61). The most well-studied function of *VHL* involves its role in angiogenesis (62, 63). When cells are well-oxygenated, prolyl hydroxylation of hypoxia inducible factor 1, alpha subunit (*HIFα*) proteins leads to their binding to *VHL*. *VHL* then recruits an ubiquitin ligase complex that leads to the ubiquitination and subsequent degradation of HIFα. When *VHL* is inactivated, HIFα proteins are stabilized, resulting in the expression of numerous genes that stimulate angiogenesis even when cells are well-oxygenated.

There are at least two ways in which *VHL* mutations might stimulate SCA formation. First, it has been noted that there is a rich capillary network within SCAs, presumably a result of the abnormal activation of HIFα. This network could disturb local hemodynamics, facilitating the production of cyst fluid, and the increased local concentration of growth factors could stimulate epithelial cell proliferation (21). A second possibility involves the stabilization of microtubules, which is a well-documented but less extensively studied function of the VHL protein (64, 65). In the absence of *VHL*, primary cilia are absent or defective (66). In view of abundant evidence linking certain types of cysts to defects in primary cilia, it has been suggested that the microtubule stabilization function of *VHL* is key to its role in suppressing cysts (66). Several mouse models in which the *VHL* gene has been inactivated develop various cysts (although not SCAs) (67–70), suggesting fertile avenues for future research on this topic.

Our results also have potentially important diagnostic implications. As mentioned previously in this report, the distinction among various types of cysts before surgical intervention is critically important for patient management (1, 2, 9–17). Cyst fluid can be readily obtained from such patients and subjected to analytical assays (22, 23, 26, 27, 71–73). Our results show that the analysis of only five genes (*VHL*, *RNF43*, *CTNNB1*, *GNAS*, and *KRAS*) can usually distinguish among cyst types (Table 1): All eight SCAs had intragenic mutations of *VHL* or LOH in or adjacent to *VHL* and did not contain mutations of the other four genes; all eight IPMNs had alterations of *RNF43*, *GNAS*, or *KRAS* and never had *VHL* or *CTNNB1* mutations; MCNs always harbored *KRAS* or *RNF43* mutations but never contained *GNAS*, *CTNNB1*, or *VHL* mutations; and SPNs always contained *CTNNB1* mutations and never contained mutations of the other four genes. When combined with clinical and radiological data, the molecular genetic analysis of cyst fluid could thereby lead to more accurate diagnosis. For IPMNs and MCNs, it will be important to determine whether the number and type of genetic alterations in *GNAS*, *RNF43*, and other genes can be used to help gauge the risk for progression to invasive cancers. The examination of a large number of cyst fluid samples from patients with all four cyst types will be required to determine the added value of molecular genetic analyses for these and other diagnostic purposes.

Materials and Methods

Patients and Specimens. The present study was approved by the Institutional Review Boards of the Johns Hopkins Medical Institutions, Memorial Sloan–Kettering Cancer Center, Wayne State University, Emory University, and the University of Indiana. DNA was purified and libraries were prepared as described (74). Captured DNA libraries were sequenced with the Illumina GAIIx/HiSeq Genome Analyzer, using one lane per sample, yielding 150 (2×75) base pairs from the final library fragments. Sequencing reads were analyzed and aligned to human genome hg18 with the Eland algorithm in CASAVA 1.7 software (Illumina). Mutations were confirmed as described in ref. 41 using the primers listed in Dataset S6. Further details are provided in *SI Materials and Methods*.

ACKNOWLEDGMENTS. We thank J. Schaeffer, J. Ptak, N. Silliman, M. Whalen, and L. Dobbyn for expert technical assistance. This work was supported by the Lustgarten Foundation for Pancreatic Cancer Research; the Virginia and D. K. Ludwig Fund for Cancer Research; The Sol Goldman Pancreatic Cancer Research Center; the Joseph L. Rabinowitz Fund; the Michael Rolfe Foundation; the Stringer Foundation; the family of Ted and Julie Smith; the Indiana Genomics Initiative of Indiana University, which is supported, in part, by Lilly Endowment, Inc.; the J. C. Monastra Foundation; Swim Across America; National Science Foundation Grant DBI-1845275; National Institutes of Health Grants CA 62924, CA 57345, CA 152432, and CA 43460; and National Cancer Institute Contracts N01-CN-43302, N01-CN-43309, and NCI grant P01CA134292.

1. Garcea G, et al. (2008) Cystic lesions of the pancreas. A diagnostic and management dilemma. *Pancreatology* 8:236–251.
2. Tanaka M (2011) Controversies in the management of pancreatic IPMN. *Nat Rev Gastroenterol Hepatol* 8:56–60.
3. Kimura W, Nagai H, Kuroda A, Muto T, Esaki Y (1995) Analysis of small cystic lesions of the pancreas. *Int J Pancreatol* 18:197–206.
4. Zhang XM, Mitchell DG, Dohke M, Holland GA, Parker L (2002) Pancreatic cysts: Depiction on single-shot fast spin-echo MR images. *Radiology* 223:547–553.
5. de Jong K, et al. (2010) High prevalence of pancreatic cysts detected by screening magnetic resonance imaging examinations. *Clin Gastroenterol Hepatol* 8:806–811.
6. Lee KS, Sekhar A, Rofsky NM, Pedrosa I (2010) Prevalence of incidental pancreatic cysts in the adult population on MR imaging. *Am J Gastroenterol* 105:2079–2084.
7. Spinelli KS, et al. (2004) Cystic pancreatic neoplasms: Observe or operate. *Ann Surg* 239:651–657, discussion 657–659.
8. Laffan TA, et al. (2008) Prevalence of unsuspected pancreatic cysts on MDCT. *AJR Am J Roentgenol* 191:802–807.
9. Allen PJ, Brennan MF (2007) The management of cystic lesions of the pancreas. *Adv Surg* 41:211–228.
10. Op de Beeck B, et al. (2007) Management of cystic pancreatic masses. *JBR-BTR* 90: 482–486.
11. Carpizo DR, Allen PJ, Brennan MF (2008) Current management of cystic neoplasms of the pancreas. *Surgeon* 6:298–307.
12. Katz MH, et al. (2008) Diagnosis and management of cystic neoplasms of the pancreas: An evidence-based approach. *J Am Coll Surg* 207:106–120.
13. Waters JA, Schmidt CM (2008) Intraductal papillary mucinous neoplasm—When to resect? *Adv Surg* 42:87–108.
14. Brugge WR (2008) Management and outcomes of pancreatic cystic lesions. *Dig Liver Dis* 40:854–859.
15. Degen L, Wiesner W, Beglinger C (2008) Cystic and solid lesions of the pancreas. *Best Pract Res Clin Gastroenterol* 22:91–103.
16. Basturk O, Coban I, Adsay NV (2009) Pancreatic cysts: Pathologic classification, differential diagnosis, and clinical implications. *Arch Pathol Lab Med* 133:423–438.
17. Matthaei H, Schulick RD, Hruban RH, Maitra A (2011) Cystic precursors to invasive pancreatic cancer. *Nat Rev Gastroenterol Hepatol* 8:141–150.
18. Hruban RH, Maitra A, Kern SE, Goggins M (2007) Precursors to pancreatic cancer. *Gastroenterol Clin North Am* 36:831–849, vi.
19. Sohn TA, et al. (2004) Intraductal papillary mucinous neoplasms of the pancreas: An updated experience. *Ann Surg*, 239:788–797; discussion 797–799.
20. Reddy S, Wolfgang CL (2009) Solid pseudopapillary neoplasms of the pancreas. *Adv Surg* 43:269–282.
21. Thirabanjasak D, Basturk O, Altinel D, Cheng JD, Adsay NV (2009) Is serous cystadenoma of the pancreas a model of clear-cell-associated angiogenesis and tumorigenesis? *Pancreatology* 9:182–188.
22. Hammel P (2002) Role of tumor markers in the diagnosis of cystic and intraductal neoplasms. *Gastrointest Endosc Clin N Am* 12:791–801.
23. van der Waaij LA, van Dullemen HM, Porte RJ (2005) Cyst fluid analysis in the differential diagnosis of pancreatic cystic lesions: A pooled analysis. *Gastrointest Endosc* 62:383–389.
24. Khalid A, Brugge W (2007) ACG practice guidelines for the diagnosis and management of neoplastic pancreatic cysts. *Am J Gastroenterol* 102:2339–2349.
25. Vazquez-Sequeiros E (2007) Endoscopic ultrasound and fine needle aspiration in inflammatory and cystic pancreatic pathology. *Minerva Med* 98:357–360.
26. Anderson MA, Kwon RS, Scheiman JM (2009) PANDA cyst-fluid analysis: Eats, shoots and leaves? *Gastrointest Endosc* 69:1103–1105.
27. Khalid A, et al. (2009) Pancreatic cyst fluid DNA analysis in evaluating pancreatic cysts: A report of the PANDA study. *Gastrointest Endosc* 69:1095–1102.
28. Maker AV (2011) Cyst fluid interleukin-1beta (IL1beta) levels predict the risk of carcinoma in intraductal papillary mucinous neoplasms of the pancreas. *Clin Cancer Res* 17:1502–1508.
29. Wang TL, et al. (2002) Digital karyotyping. *Proc Natl Acad Sci USA* 99:16156–16161.
30. Jiao Y, et al. (2011) DAXX/ATRX, MEN1, and mTOR pathway genes are frequently altered in pancreatic neuroendocrine tumors. *Science* 331:1199–1203.
31. Jones S, et al. (2010) Frequent mutations of chromatin remodeling gene ARID1A in ovarian clear cell carcinoma. *Science* 330:228–231.
32. Jones S, et al. (2008) Core signaling pathways in human pancreatic cancers revealed by global genomic analyses. *Science* 321:1801–1806.
33. Wainszelbaum MJ, et al. (2008) The hominoid-specific oncogene TBC1D3 activates Ras and modulates epidermal growth factor receptor signaling and trafficking. *J Biol Chem* 283:13233–13242.
34. Stenmark H (2009) Rab GTPases as coordinators of vesicle traffic. *Nat Rev Mol Cell Biol* 10:513–525.
35. Nakamura T, et al. (1992) A novel transcriptional unit of the tre oncogene widely expressed in human cancer cells. *Oncogene* 7:733–741.
36. Pei L, et al. (2002) PRC17, a novel oncogene encoding a Rab GTPase-activating protein, is amplified in prostate cancer. *Cancer Res* 62:5420–5424.
37. Linehan WM, et al. (2009) Hereditary kidney cancer: Unique opportunity for disease-based therapy. *Cancer* 115(Suppl):2252–2261.
38. Herman JG, et al. (1994) Silencing of the VHL tumor-suppressor gene by DNA methylation in renal carcinoma. *Proc Natl Acad Sci USA* 91:9700–9704.
39. Choyke PL, et al. (1995) von Hippel-Lindau disease: Genetic, clinical, and imaging features. *Radiology* 194:629–642.
40. Neumann HP, et al. (1991) Pancreatic lesions in the von Hippel-Lindau syndrome. *Gastroenterology* 101:465–471.
41. Wu J, et al. (2011) Recurrent GNAS mutations define an unexpected pathway for pancreatic cyst development. *Sci Transl Med* 3:92ra66.
42. Kitago M, et al. (2004) Comparison of K-ras point mutation distributions in intraductal papillary-mucinous tumors and ductal adenocarcinoma of the pancreas. *Int J Cancer* 110:177–182.
43. Almoguera C, et al. (1988) Most human carcinomas of the exocrine pancreas contain mutant c-K-ras genes. *Cell* 53:549–554.
44. Kinzler KW, Vogelstein B (1996) Lessons from hereditary colorectal cancer. *Cell* 87: 159–170.
45. Carter H, et al. (2009) Cancer-specific high-throughput annotation of somatic mutations: Computational prediction of driver missense mutations. *Cancer Res* 69: 6660–6667.
46. Sugiura T, Yamaguchi A, Miyamoto K (2008) A cancer-associated RING finger protein, RNF43, is a ubiquitin ligase that interacts with a nuclear protein, HAP95. *Exp Cell Res* 314:1519–1528.
47. Yagyu R, et al. (2004) A novel oncoprotein RNF43 functions in an autocrine manner in colorectal cancer. *Int J Oncol* 25:1343–1348.
48. Khalid A, Finkelstein S, McGrath K (2004) Molecular diagnosis of solid and cystic lesions of the pancreas. *Gastroenterol Clin North Am* 33:891–906.
49. Chin L, Hahn WC, Getz G, Meyerson M (2011) Making sense of cancer genomic data. *Genes Dev* 25:534–555.
50. Stratton MR (2011) Exploring the genomes of cancer cells: Progress and promise. *Science* 331:1553–1558.
51. Parsons DW, et al. (2011) The genetic landscape of the childhood cancer medulloblastoma. *Science* 331:435–439.
52. Clevers H (2006) Wnt/beta-catenin signaling in development and disease. *Cell* 127: 469–480.
53. Nelson WJ, Nusse R (2004) Convergence of Wnt, beta-catenin, and cadherin pathways. *Science* 303:1483–1487.
54. Verheyen EM, Gottardi CJ (2010) Regulation of Wnt/beta-catenin signaling by protein kinases. *Dev Dyn* 239:34–44.
55. Morin PJ, et al. (1997) Activation of beta-catenin-Tcf signaling in colon cancer by mutations in beta-catenin or APC. *Science* 275:1787–1790.
56. Rubinfeld B, et al. (1997) Stabilization of beta-catenin by genetic defects in melanoma cell lines. *Science* 275:1790–1792.
57. Tanaka Y, et al. (2001) Frequent beta-catenin mutation and cytoplasmic/nuclear accumulation in pancreatic solid-pseudopapillary neoplasm. *Cancer Res* 61:8401–8404.
58. Abraham SC, et al. (2002) Solid-pseudopapillary tumors of the pancreas are genetically distinct from pancreatic ductal adenocarcinomas and almost always harbor beta-catenin mutations. *Am J Pathol* 160:1361–1369.
59. Vogelstein B, Kinzler KW (2004) Cancer genes and the pathways they control. *Nat Med* 10:789–799.
60. Shinada K, et al. (2011) RNF43 interacts with NEDL1 and regulates p53-mediated transcription. *Biochem Biophys Res Commun* 404:143–147.
61. Latif F, et al. (1993) Identification of the von Hippel-Lindau disease tumor suppressor gene. *Science* 260:1317–1320.
62. Semenza GL (2011) Hypoxia-inducible factor 1: Regulator of mitochondrial metabolism and mediator of ischemic preconditioning. *Biochim Biophys Acta* 1813: 1263–1268.
63. Kaelin WG, Jr. (2008) The von Hippel-Lindau tumour suppressor protein: O2 sensing and cancer. *Nat Rev Cancer* 8:865–873.
64. Hergovich A, Lisztwan J, Barry R, Ballschmieter P, Krek W (2003) Regulation of microtubule stability by the von Hippel-Lindau tumour suppressor protein pVHL. *Nat Cell Biol* 5:64–70.
65. Lolkema MP, et al. (2004) The von Hippel-Lindau tumor suppressor protein influences microtubule dynamics at the cell periphery. *Exp Cell Res* 301:139–146.
66. Thoma CR, et al. (2007) pVHL and GSK3beta are components of a primary cilium-maintenance signalling network. *Nat Cell Biol* 9:588–595.
67. Rankin EB, Tomaszewski JE, Haase VH (2006) Renal cyst development in mice with conditional inactivation of the von Hippel-Lindau tumor suppressor. *Cancer Res* 66:2576–2583.
68. Frew IJ, et al. (2008) pVHL and PTEN tumour suppressor proteins cooperatively suppress kidney cyst formation. *EMBO J* 27:1747–1757.
69. Shen HC, et al. (2009) Deciphering von Hippel-Lindau (VHL/Vhl)-associated pancreatic manifestations by inactivating Vhl in specific pancreatic cell populations. *PLoS ONE* 4: e4897.
70. Fu L, Wang G, Shevchuk MM, Nanus DM, Gudas LJ (2011) Generation of a Mouse Model of Von Hippel-Lindau Kidney Disease Leading to Renal Cancers by Expression of a Constitutively Active Mutant of HIF1α. *Cancer Res* 71:6848–6856.
71. Sawhney MS, et al. (2009) Comparison of carcinoembryonic antigen and molecular analysis in pancreatic cyst fluid. *Gastrointest Endosc* 69:1106–1110.
72. Maker AV, et al. (2011) Cyst fluid interleukin-1beta (IL1beta) levels predict the risk of carcinoma in intraductal papillary mucinous neoplasms of the pancreas. *Clin Cancer Res* 17:1502–1508.
73. Mertz H (2011) K-ras mutations correlate with atypical cytology and elevated CEA levels in pancreatic cystic neoplasms. *Dig Dis Sci* 56:2197–2201.
74. Bettegowda C, et al. (2011) Mutations in CIC and FUBP1 contribute to human oligodendroglioma. *Science* 333:1453–1455.